16

Some Nonclassical Hyperbolic Problems

In the previous chapters on nonlinear problems we have concentrated on *classical* systems of conservation laws for which the wave structure is relatively simple. In particular, we have assumed that the system is strictly hyperbolic (so that there are m distinct integral curves through each point of phase space), and that each characteristic field is either linearly degenerate or genuinely nonlinear (so that the eigenvalue is constant or varies monotonically along each integral curve). Many important systems of equations satisfy these conditions, including the shallow water equations and the Euler equations for an ideal gas, as well as linear systems such as acoustics. However, there are other important applications where one or both of these conditions fail to hold, including some problems arising in nonlinear elasticity, porous-media flow, phase transition, and magnetohydrodynamics (MHD). In this chapter we explore a few of the issues that can arise with more general systems. This is only an introduction to some of the difficulties, aimed primarily at explaining why the above assumptions lead to simplifications.

We start by considering scalar conservation laws with nonconvex flux functions (which fail to be genuinely nonlinear because $f''(q)$ vanishes at one or more points). This gives a good indication of the complications that arise also in systems of more equations that fail to be genuinely nonlinear. Then in Section 16.2 we will investigate the complications that can arise if a system is not strictly hyperbolic, i.e., if some of the wave speeds coincide at one or more points in phase space. In Section 16.3 we go even further and see what can happen if the system fails to be (strongly) hyperbolic at some points, either because the matrix is not diagonalizable or because the eigenvalues are not real.

In Section 16.4 we consider nonlinear conservation laws with spatially varying flux functions $f(q, x)$, analogous to the variable-coefficient linear systems considered in Chapter 9. Finally, Section 16.5 contains some discussion of nonconservative nonlinear hyperbolic problems.

16.1 Nonconvex Flux Functions

For the scalar conservation laws studied thus far, the flux function $f(q)$ was assumed to be a convex or concave function of q, meaning that $f''(q)$ has the same sign everywhere. For the traffic flux (11.6) it is constant and negative everywhere when $u_{\max} > 0$. Burgers' equation is convex, since $f''(u) \equiv 1$. As shorthand we typically refer to all such genuinely nonlinear problems as *convex*.

Convexity is important because it means that the characteristic speed $f'(q)$ is varying monotonically as q varies. In solving the Riemann problem with $q_l > q_r$ (Figure 11.3), we obtain a smooth rarefaction wave with cars spreading out, since $f'(q)$ is nondecreasing as x increases. On the other hand if $q_l < q_r$ as in Figure 11.2, then the Riemann solution consists of a shock joining these two values. If the function $f(q)$ is not convex, then the Riemann solution may be more complicated and can involve both shock and rarefaction waves.

16.1.1 Two-Phase Flow and the Buckley–Leverett Equation

As an example where nonconvex flux functions arise, we study a simple model for two-phase fluid flow in a porous medium. One application is to oil-reservoir simulation. When an underground source of oil is tapped, a certain amount of oil flows out on its own due to high pressure in the reservoir. After the flow stops, there is typically a large amount of oil still in the ground. One standard method of subsequent *secondary recovery* is to pump water into the oil field through some wells, forcing oil out through others. In this case the two phases are oil and water, and the flow takes place in a porous medium of rock or sand.

We can consider a one-dimensional model problem in which oil in a tube of porous material is displaced by water pumped in through one end. Let $q(x, t)$ represent the fraction of fluid that is water (the *water saturation*), so that $0 \le q \le 1$, and $1 - q(x, t)$ is the fraction that is oil. If we take initial data

$$q(x, 0) = \begin{cases} 1 & \text{if } x < 0, \\ 0 & \text{if } x > 0, \end{cases} \tag{16.1}$$

so that water is to the left and oil to the right, and take a positive flow rate (pumping water in from the left), then we expect the water to displace the oil. Our first guess might be that the sharp interface between pure water ($q = 1$) and pure oil ($q = 0$) will be maintained and simply advect with constant velocity. Instead, however, one observes a sharp interface between pure oil and some mixed state $q = q^* < 1$, followed by a region in which both oil and water are present ($q^* < q < 1$). Mathematically we will see that this corresponds to a shock wave followed by a rarefaction wave.

Since both fluids are essentially incompressible, we expect the total flux of fluid to be the same past any point in the tube. In regions of pure oil or pure water the velocity must thus be the same, and we will take this value to be 1. However, in regions where both fluids are present, they may be moving at different average velocities. It is this behavior that leads to the interesting mathematical structure. Physically this arises from the fact that a porous medium consists of a solid material with many pores or minute cracks through which the fluids slowly seep. Particles of the oil are initially bound to the solid substrate and must be displaced by the water molecules. The fact that oil and water do not mix (the fluids are *immiscible*) means that surface tension effects between the two fluids are crucial on the small length scales of the pores, and can inhibit the movement of water into the smallest pores filled with oil. Regions where $0 < q < 1$ correspond to regions where some of the oil is still bound to the substrate and is stationary, so the average velocity of oil molecules may be considerably less than the average velocity of water molecules.

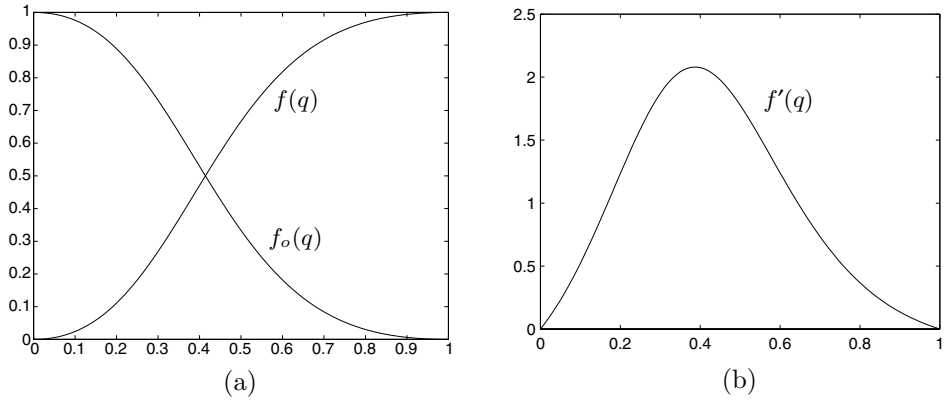

Fig. 16.1. (a) Flux functions (16.2) for the Buckley–Leverett equation, as functions of the water saturation q. (b) The characteristic speed $f'(q)$. Shown for $a = 1/2$ in (16.2).

Buckley and Leverett proposed a simple model for this complex situation in which the flux of water and oil are each given by expressions that depend on the saturation of the fluid:

$$\begin{aligned} &\text{flux of water:} \quad f(q) = \frac{q^2}{q^2 + a(1-q)^2}; \\ &\text{flux of oil:} \quad f_o(q) = \frac{a(1-q)^2}{q^2 + a(1-q)^2}. \end{aligned} \tag{16.2}$$

Here $a < 1$ is a constant. Each of the fluxes can be viewed as the product of the saturation of the phase with the average velocity of the phase. In each case the idea is that the average velocity approaches 0 as the saturation goes to 0 (the few molecules present are bound to the substrate) and approaches 1 as the saturation goes to 1 (since the fluid as a whole is flowing at this rate). The fact that $a < 1$ arises from the fact that oil flows less easily than water. So if $q = 1 - q = 0.5$, for example, we expect more water than oil to be flowing. We take $a = 1/2$ in the figures here. Note that $f(q) + f_o(q) \equiv 1$, so that the total fluid flux is the same everywhere, as required by incompressibility. Figure 16.1(a) shows these fluxes as a function of q.

We only need to solve for q, the water saturation, and so we can solve a scalar conservation law

$$q_t + f(q)_x = 0$$

with the flux $f(q)$ given by (16.2). Note that this flux is nonconvex, with a single inflection point. Figure 16.1(b) shows the characteristic speed

$$f'(q) = \frac{2aq(1-q)}{[q^2 + a(1-q)^2]^2},$$

which has a maximum at the point of inflection.

Now consider the Riemann problem with initial states $q_l = 1$ and $q_r = 0$. By following characteristics, we can construct the triple-valued solution shown in Figure 16.2(a). Note that the characteristic velocities are $f'(q)$, so that the profile of this bulge, seen here at time t, is simply the graph of $tf'(q)$ turned sideways.

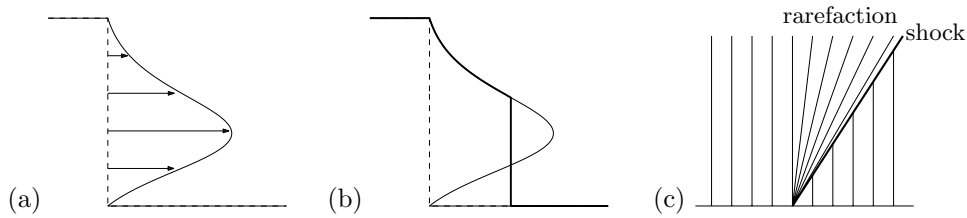

Fig. 16.2. Riemann solution for the Buckley–Leverett equation. (a) Triple-valued solution obtained by following characteristics. (b) Insertion of an area-preserving shock. (c) Structure in the x–t plane.

We can now use the equal-area rule to replace this triple-valued solution by a correct shock. The resulting weak solution is shown in Figure 16.2(b), along with the characteristics in Figure 16.2(c). The postshock value q^* is constant in time (Exercise 16.2), and so is the shock speed

$$s = \frac{f(q^*) - f(q_r)}{q^* - q_r} = \frac{f(q^*)}{q^*}. \tag{16.3}$$

This is to be expected, since the solution to the Riemann problem is still self-similar in the nonconvex case.

Note the physical interpretation of the solution shown in Figure 16.2. As the water moves in, it displaces a certain fraction q^* of the oil immediately. Behind the shock, there is a mixture of oil and water, with less and less oil as time goes on. At a production well (at the point $x = 1$, say), one obtains pure oil until the shock arrives, followed by a mixture of oil and water with diminishing returns as time goes on. It is impossible to recover all of the oil in finite time by this technique.

Note that the Riemann solution involves both a shock and a rarefaction wave and is called a *compound wave*. If $f(q)$ had more inflection points, the solution might involve several shocks and rarefactions (as in Example 16.1 below).

Here we only consider scalar nonconvex problems. For a nonlinear system of equations, similar behavior can arise in any nonlinear field that fails to be genuinely nonlinear (see Section 13.8.4). This arises, for example, in the one-dimensional elasticity equations (2.97) with a nonconvex stress–strain relation. See, e.g., [483], [484].

16.1.2 Solving Nonconvex Riemann Problems

To determine the correct weak solution to a nonconvex scalar conservation law, we need an admissibility criterion for shock waves that applies in this case. A more general form of the entropy condition (11.40), due to Oleinik [347], applies also to nonconvex scalar flux functions f:

Entropy Condition 16.1 (Oleinik). A weak solution $q(x, t)$ is the vanishing-viscosity solution to a general scalar conservation law if all discontinuities have the property that

$$\frac{f(q) - f(q_l)}{q - q_l} \geq s \geq \frac{f(q) - f(q_r)}{q - q_r} \tag{16.4}$$

for all q between q_l and q_r.

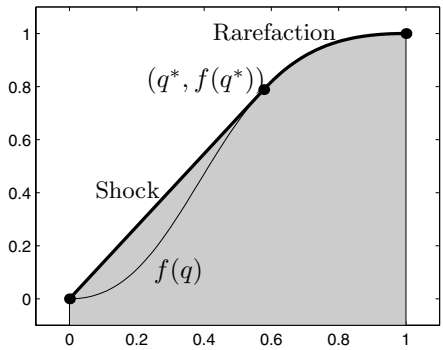

Fig. 16.3. Convex-hull construction of the Riemann solution for the Buckley–Leverett equation with $q_l = 1$ and $q_r = 0$. The shaded region is the convex hull of the set of points lying below the graph of $f(q)$.

For convex f, this requirement reduces to (11.40). (Note that this may not always be the correct admissibility condition to apply; see [285] for a nonconvex traffic-flow example where the vanishing-viscosity criterion would select the wrong solution.)

Convex-Hull Construction

The entropy-satisfying solution to a nonconvex Riemann problem can be determined from the graph of $f(q)$ in a simple manner. If $q_r < q_l$, then construct the *convex hull* of the set $\{(q, y) : q_r \le q \le q_l \text{ and } y \le f(q)\}$. The convex hull is the smallest convex set containing the original set. This is shown in Figure 16.3 for the case $q_l = 1, q_r = 0$.

If we look at the upper boundary of this set, we see that it is composed of a straight line segment from $(0, 0)$ to $(q^*, f(q^*))$ and then follows $y = f(q)$ up to $(1, 1)$. The point of tangency q^* is precisely the postshock value. The straight line represents a shock jumping from $q = 0$ to $q = q^*$, and the segment where the boundary follows $f(q)$ is the rarefaction wave. This works more generally for any two states (provided $q_l > q_r$) and for any f.

Note that the slope of the line segment is equal to the shock speed (16.3). The fact that this line is tangent to the curve $f(q)$ at q^* means that $s = f'(q^*)$, the shock moves at the same speed as the characteristics at this edge of the rarefaction fan, as seen in Figure 16.2(c).

If the shock were connected to some point $\hat{q} < q^*$, then the shock speed $f(\hat{q})/\hat{q}$ would be less than $f'(\hat{q})$, leading to a triple-valued solution. On the other hand, if the shock were connected to some point above q^*, then the entropy condition (16.4) would be violated. This explains the tangency requirement, which comes out naturally from the convex-hull construction. The same construction works for any $q_r < q_l$ lying in $[0, 1]$.

If $q_l < q_r$, then the same idea works, but we look instead at the convex hull of the set of points *above* the graph, $\{(q, y) : q_l \le q \le q_r \text{ and } y \ge f(q)\}$, as illustrated in Example 16.1.

Note that if f is convex, then the convex hull construction gives either a single line segment (single shock) if $q_l > q_r$ or the function f itself (single rarefaction) if $q_l < q_r$.

Example 16.1. Figure 16.4(a) shows another example for the flux function $f(q) = \sin(q)$ with $q_l = \pi/4$ and $q_r = 15\pi/4$. The shaded region is the convex hull of the set of points *above* this curve, since $q_l < q_r$. The lower boundary of this set shows the structure of

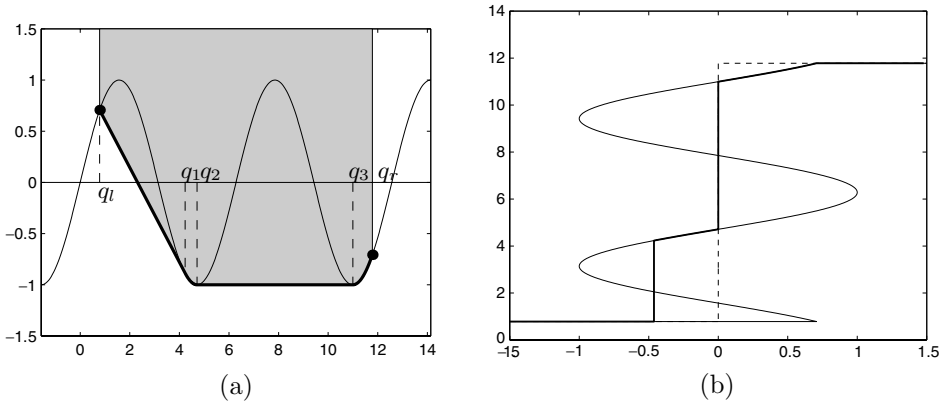

Fig. 16.4. Solving the scalar Riemann problem with a nonconvex flux function $f(q) = \sin(q)$. (a) The flux function $f(q)$. The lower boundary of the convex hull determines the structure of the Riemann solution. (b) The solution $q(x, t)$ as a function of x at time $t = 1$ (heavy line) together with the initial data (dashed line) and the multivalued solution that would be obtained by following characteristics (light line).

the Riemann solution: a shock from q_l to some value q_1, a rarefaction wave from q_1 to $q_2 = 3\pi/2$, a stationary shock from q_2 to $q_3 = 7\pi/2$, and finally a rarefaction from q_3 to q_r. The value of $q_1 \approx 4.2316$ can be found by solving the nonlinear equation

$$\frac{\sin(q_1) - \sin(\pi/4)}{q_1 - \pi/4} = \cos(q_1),$$

since the slope of the line segment from q_l to q_1 must match $f'(q_1)$. Figure 16.4(b) shows the Riemann solution together with the multivalued solution that would be obtained by following characteristics. Note that the equal-area rule of Section 11.7 again applies to the shocks.

Osher's Solution

Osher [349] found a simple representation for the entropy-satisfying similarity solution $q(x, t) = \tilde{q}(x/t)$ for a general nonconvex scalar Riemann problem with arbitrary data q_l and q_r. Let $\xi = x/t$, and set

$$G(\xi) = \begin{cases} \min\limits_{q_l \le q \le q_r} (f(q) - \xi q) & \text{if } q_l \le q_r, \\ \max\limits_{q_r \le q \le q_l} (f(q) - \xi q) & \text{if } q_r \le q_l. \end{cases} \tag{16.5}$$

Then it can be shown that $\tilde{q}(\xi)$ satisfies the equation

$$f(\tilde{q}(\xi)) - \xi \tilde{q}(\xi) = G(\xi). \tag{16.6}$$

In other words, for any given value of ξ, $\tilde{q}(\xi)$ is the value of q for which $f(q) - \xi q$ is minimized or maximized, depending on whether $q_l \le q_r$ or $q_r \le q_l$. We can also write this

as

$$\tilde{q}(\xi) = \begin{cases} \operatorname{argmin}_{q_l \le q \le q_r} [f(q) - \xi q] & \text{if } q_l \le q_r, \\ \operatorname{argmax}_{q_r \le q \le q_l} [f(q) - \xi q] & \text{if } q_r \le q_l. \end{cases} \tag{16.7}$$

In general the argmin function returns the argument that minimizes the expression, and similarly for argmax.

Note that for any fixed q_0 we can replace $f(q) - \xi q$ by $[f(q) - f(q_0)] - \xi(q - q_0)$ in (16.7). Often an appropriate choice of q_0 (e.g., q_l or q_r) makes it easier to interpret this expression, since it is intimately related to the Rankine–Hugoniot jump condition (11.21).

Differentiating the expression (16.6) with respect to ξ gives

$$[f'(\tilde{q}(\xi)) - \xi]\tilde{q}'(\xi) - \tilde{q}(\xi) = G'(\xi). \tag{16.8}$$

Along every ray $x/t = \xi$ in the Riemann solution we have either $\tilde{q}'(\xi) = 0$ or else $f'(\tilde{q}(\xi)) = \xi$ (in a rarefaction wave), and hence (16.8) reduces to an expression for $\tilde{q}(\xi)$:

$$\tilde{q}(\xi) = -G'(\xi). \tag{16.9}$$

This gives the general solution to the Riemann problem.

The equation (16.6) is particularly useful in the case $\xi = 0$, for which it yields the value $f(\tilde{q}(0))$ along $x/t = 0$. This is the flux value $f(q^{\Downarrow}(q_l, q_r))$ needed in implementing Godunov's method and generalizations. When $\xi = 0$, (16.6) reduces to

$$f(q^{\Downarrow}(q_l, q_r)) = f(\tilde{q}(0)) = G(0) = \begin{cases} \min_{q_l \le q \le q_r} f(q) & \text{if } q_l \le q_r, \\ \max_{q_r \le q \le q_l} f(q) & \text{if } q_r \le q_l. \end{cases} \tag{16.10}$$

We have already seen this formula for the special case of a convex flux function in (12.4).

16.1.3 Finite Volume Methods for Nonconvex Problems

Finite volume methods for nonconvex problems (see Section 16.1) can be developed using the same approach as for convex problems. To apply Godunov's method to a scalar nonconvex problem, we must compute the flux $F_{i-1/2} = f(Q^{\Downarrow}_{i-1/2})$, where $Q^{\Downarrow}_{i-1/2}$ is the value along $x/t = 0$ in the entropy-satisfying solution to the Riemann problem between states Q_{i-1} and Q_i. This is easily computed using the general formula (16.10), resulting in (12.4). As usual, this flux can be converted into fluctuations $\mathcal{A}^{\pm}\Delta Q_{i-1/2}$ using (12.6).

To apply a high-resolution method, we also need to define one or more waves and corresponding speeds. Since the Riemann solution may consist of several waves in the nonconvex case, one might think it necessary to handle each wave separately. In fact it appears to be sufficient to use a single wave and the corresponding Rankine–Hugoniot speed,

$$\mathcal{W}_{i-1/2} = Q_i - Q_{i-1}, \qquad s_{i-1/2} = \frac{f(Q_i) - f(Q_{i-1})}{Q_i - Q_{i-1}}.$$

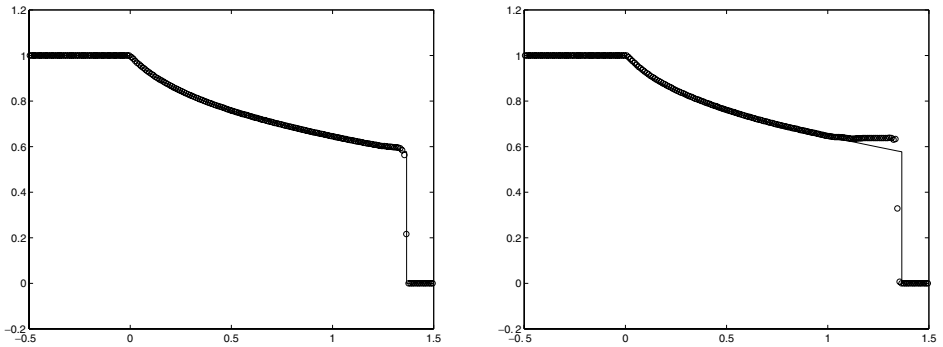

Fig. 16.5. (a) Computed solution to the Buckley–Leverett problem at time $t = 1$ using CLAWPACK with sufficiently small time steps that the Courant number is less than 1. (b) Entropy-violating solution obtained with CLAWPACK when the true Courant number is greater than 1. `[claw/book/chap16/bucklev]`

In computing the fluctuations an entropy fix must be included, as in the convex case, if the solution contains a transonic rarefaction. It is also important to insure that the Courant number is less than 1. Note that in computing the Courant number we must use the formula

$$\text{Courant number} = \max \left| \frac{\Delta t}{\Delta x} f'(q) \right|,$$

where we maximize over the entire range of q that appears in the solution, e.g., over [0, 1] for the Buckley–Leverett example used above. For nonconvex problems this may be larger than values of $|s_{i-1/2}|\Delta t/\Delta x$ that arise in the course of solving the problem numerically (which is how CLAWPACK estimates the Courant number). This is because the steepest part of the flux function may be in regions that are embedded in shocks and not sampled by the cell averages arising in the problem.

Figure 16.5(a) shows a computed solution to the Buckley–Leverett equation using a high-resolution method of CLAWPACK with a time step that satisfies the CFL condition. Figure 16.5(b) shows a CLAWPACK computation with the parameter values

```
cflv(1) = 1.0,
cflv(2) = 0.8.
```

This aims for a Courant number of 0.8 and forces a step to be retaken whenever the observed Courant number is greater than 1.0. The method fails to produce the correct solution, because the actual Courant number is greater than the estimate used in CLAWPACK, and the time steps being used do not in fact satisfy the CFL condition. The solution obtained does approximate a weak solution, but one in which the shock jumps from $q = 0$ to a value greater than the q^* shown in Figure 16.3, and hence propagates at a speed that is slower than the characteristic speed at some points in between.

See `[claw/book/chap16/bucklev]` for the CLAWPACK implementation of the Buckley–Leverett equation, and `[claw/book/chap16/fsin]` for another example, the nonconvex flux function shown in Figure 16.4(a).

16.2 Nonstrictly Hyperbolic Problems

In general we have assumed that the systems we deal with are strictly hyperbolic, meaning that the eigenvalues λ^p of the Jacobian matrix are distinct. In this section we will see why this is significant and briefly explore what can happen if the system fails to be strictly hyperbolic (in which case it is called *nonstrictly hyperbolic*). We will only scratch the surface of this interesting topic, which is important in many applications where some of the consequences are still poorly understood and the subject of current research.

Recall that a matrix with distinct eigenvalues must have a one-dimensional eigenspace associated with each eigenvalue. If the Jacobian matrix $f'(q)$ has distinct eigenvalues at every point $q \in \mathbb{R}^m$, then at every point in state space there are m distinct eigendirections, which form a basis for $\mathbb{R}^m$. The integral curves and Hugoniot loci are tangent to these eigenvectors. From this it can be shown using the implicit-function theorem that the Riemann problem can be uniquely solved for any two states q_l and q_r that are sufficiently close together (see e.g., [263]). This does not necessarily mean that the Riemann problem can be solved globally for any q_l and q_r, but at least locally these curves foliate state space in an organized manner.

Now suppose the system is not strictly hyperbolic and at some point q_0 the Jacobian $f'(q_0)$ has a repeated eigenvalue. The *algebraic multiplicity* of this eigenvalue is the number of times it is repeated as a zero of the characteristic polynomial. The *geometric multiplicity* is the dimension of the linear space of eigenvectors associated with this eigenvalue, which is never greater than the algebraic multiplicity but could be less. In order for the system to be hyperbolic, the geometric multiplicity must be equal to the algebraic multiplicity, since only in this case is the Jacobian matrix diagonalizable. Otherwise the matrix is *defective*, a case discussed in Section 16.3.1.

If the system is hyperbolic but not strictly hyperbolic at q_0, then for some eigenvalue the algebraic and geometric multiplicities are equal but greater than 1. In this multidimensional eigenspace there are infinitely many directions that are eigenvectors, and this infinitude of eigendirections leads to some of the difficulties with nonstrictly hyperbolic systems. Even if this occurs only at a single point in state space, it can complicate the solution to all Riemann problems. It is possible for infinitely many integral curves or Hugoniot loci to coalesce at such a point, which is often called an *umbilic point* because of this behavior. Here we only consider some trivial examples to give an indication of how things can change. Much more interesting examples arise in various applications such as nonlinear elasticity, flow in porous media, and magnetohydrodynamics. For some examples see [51], [142], [146], [209], [210], [227], [228], [235], [237], [238], [240], [334], [335], [372], [397], [398], [460].

16.2.1 Uncoupled Advection Equations

First it is important to note that equal eigenvalues do not always lead to difficulties. In fact some physical systems (such as one-dimensional Riemann problems arising from the multidimensional Euler equations) always have repeated eigenvalues at every point in state space and yet require no special treatment.

As a simple example, suppose we model two distinct tracers being advected in a fluid moving at constant velocity $\bar{u}$, with concentrations denoted by q^1 and q^2. Then we obtain

two uncoupled advection equations

$$\begin{aligned} q_t^1 + \bar{u} q_x^1 &= 0, \\ q_t^2 + \bar{u} q_x^2 &= 0, \end{aligned} \tag{16.11}$$

which are easily solved independently. If we view this as a system, then the coefficient matrix is diagonal:

$$A = \begin{bmatrix} \bar{u} & 0 \\ 0 & \bar{u} \end{bmatrix}. \tag{16.12}$$

This matrix has eigenvalues $\lambda^1 = \lambda^2 = \bar{u}$ with all of $\mathbb{R}^2$ as the two-dimensional eigenspace; every direction is an eigendirection. Note that the solution to the Riemann problem between arbitrary states q_l and q_r consists of a single wave $\mathcal{W}^1 = q_r - q_l$ with speed $s^1 = \bar{u}$, since the Rankine–Hugoniot jump condition $A(q_r - q_l) = \bar{u}(q_r - q_l)$ is satisfied for every vector $q_r - q_l$. Every curve in state space is an integral curve of this system, but this causes no real problems.

We should note, however, that computationally it is better to use two waves

$$\mathcal{W}^1 = \begin{bmatrix} q_r^1 - q_l^1 \\ 0 \end{bmatrix}, \qquad \mathcal{W}^2 = \begin{bmatrix} 0 \\ q_r^2 - q_l^2 \end{bmatrix},$$

with equal speeds $s^1 = s^2 = \bar{u}$ when using a high-resolution method. This way the limiter is applied separately to each component of the system. Otherwise a discontinuity in q^1 in a region where the concentration q^2 is smooth would lead to a loss of accuracy in the approximation to q^2.

A similar sort of benign nonstrict hyperbolicity is seen in the two-dimensional Euler equations, as discussed in Section 18.8. If we solve a one-dimensional Riemann problem in any direction then the solution consists of four waves: two nonlinear acoustic waves and two linearly degenerate waves moving at the intermediate fluid velocity u^*. These latter waves form the contact discontinuity, across which the two initial gases are in contact. One of these waves carries a jump in density (as in the one-dimensional Euler equations), and the other carries a jump in the transverse velocity (see Section 18.8). As in the advection example above, we could view these as a single wave carrying jumps in both quantities, though computationally it may be best to keep them distinct. If we couple the Euler equations with the transport of different chemical species in the gases, then additional linearly degenerate waves will arise, moving at the same speed. The fact that these waves are linearly degenerate and the same eigenspace arises at every point in state space means that this loss of strict hyperbolicity does not lead to any mathematical or computational difficulties.

16.2.2 Uncoupled Burgers' Equations

Now consider a pair of Burgers' equations,

$$\begin{aligned} u_t + \frac{1}{2}(u^2)_x &= 0, \\ v_t + \frac{1}{2}(v^2)_x &= 0, \end{aligned} \tag{16.13}$$

for which

$$q = \begin{bmatrix} u \\ v \end{bmatrix}, \qquad f(q) = \frac{1}{2}\begin{bmatrix} u^2 \\ v^2 \end{bmatrix}, \qquad f'(q) = \begin{bmatrix} u & 0 \\ 0 & v \end{bmatrix}. \tag{16.14}$$

Again this system is easy to solve for any initial data, since the two equations are uncoupled. However, if we attempt to apply the theory developed in Chapter 13 to this system, we see that the state-space structure has become complicated by the fact that this system fails to be strictly hyperbolic along the line $u = v$. We must be careful in labeling the eigenvalues as λ^1 and λ^2, since by convention we assume $\lambda^1 \le \lambda^2$. This requires setting

$$\lambda^1 = \min(u, v), \qquad \lambda^2 = \max(u, v), \tag{16.15}$$

and hence there is a jump discontinuity in the directions r^1 and r^2 along $u = v$ as shown in Figure 16.6:

$$r^1 = \begin{cases} (1,0)^T & \text{if } u < v, \\ (0,1)^T & \text{if } u > v, \end{cases} \qquad r^2 = \begin{cases} (0,1)^T & \text{if } u < v, \\ (1,0)^T & \text{if } u > v. \end{cases} \tag{16.16}$$

For states q on the curve $u = v$, every direction is an eigendirection. This allows r^1 and r^2 to rotate by 90° as we cross this curve. While it may seem that this discontinuity is simply a result of our pedantic insistence on the ordering $\lambda^1 \le \lambda^2$, recall that in solving the Riemann problem it is crucial that we first move from q_l along an integral curve or Hugoniot locus

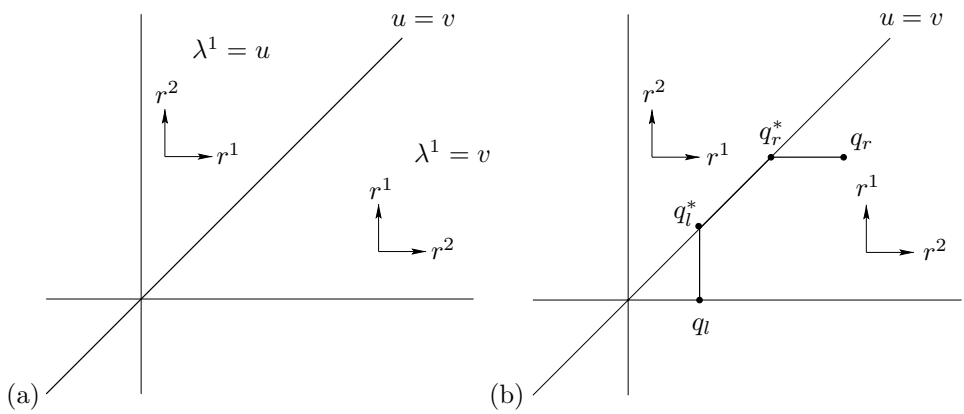

Fig. 16.6. (a) The phase plane for a pair of Burgers equations viewed as a nonstrictly hyperbolic system of equations. The eigenvalues coalesce along $u = v$. (b) Solution to a Riemann problem consisting of three segments.

corresponding to the slower speed, and then along a curve corresponding to the faster speed to reach q_r. Otherwise we cannot patch these waves together into a physically meaningful single-valued solution. For this reason the labeling is important, and the discontinuity in eigendirections across $u = v$ has consequences.

To illustrate the effect this can have on the Riemann solution, consider the data

$$q_l = \begin{bmatrix} 1 \\ 0 \end{bmatrix}, \qquad q_r = \begin{bmatrix} 3 \\ 2 \end{bmatrix}.$$

By solving the uncoupled Burgers equations, we see that $u(x, t)$ consists of a rarefaction fan for $1 \le x/t \le 3$ joining $u_l = 1$ to $u_r = 3$, while $v(x, t)$ is a rarefaction fan for $0 \le x/t \le 2$ joining $v_l = 0$ to $v_r = 2$. These two rarefaction fans partially overlap, so that the solution consists of three distinct regions:

- for $0 \le x/t \le 1$, u is constant while v is varying,
- for $1 \le x/t \le 2$, both u and v vary together,
- for $2 \le x/t \le 3$, only u varies.

The structure of this Riemann solution in state space is shown in Figure 16.6(b). The three distinct waves are clear in this picture as well. We are following an integral curve of r^1 from q_l to $q_r^* = (2, 2)^T$, and an integral curve of r^2 from $q_l^* = (1, 1)^T$ to q_r. The portion between q_l^* and q_r^* is an integral curve of both eigenvector fields.

16.2.3 Undercompressive and Overcompressive Shocks

Recall the Lax Entropy Condition 13.1. For a strictly hyperbolic system of m equations, a shock in the p-family will have $m + 1$ characteristics impinging on it: $m - p + 1$ from the left, since $\lambda^m(q_l) > \lambda^{m-1}(q_l) > \cdots > \lambda^p(q_l) > s$, and p from the right, since $s < \lambda^p(q_r) < \lambda^{p-1}(q_r) < \cdots < \lambda^1(q_r)$. This property can fail for a nonstrictly hyperbolic system. For example, consider the pair of Burgers equations (16.13) with data

$$q_l = \begin{bmatrix} 2 \\ 0 \end{bmatrix}, \qquad q_r = \begin{bmatrix} 0 \\ 2 \end{bmatrix}. \tag{16.17}$$

The solution consists of a shock in u with speed $s = 1$ and a rarefaction wave in v, with speeds ranging from 0 to 2, so that the shock is embedded in the midst of the rarefaction. The states found just to the left and right of the shock are

$$q_l^* = \begin{bmatrix} 2 \\ 1 \end{bmatrix}, \qquad q_r^* = \begin{bmatrix} 0 \\ 1 \end{bmatrix},$$

with eigenvalues $\lambda^1(q_l^*) = 1$, $\lambda^2(q_l^*) = 2$, $\lambda^1(q_r^*) = 0$, and $\lambda^2(q_r^*) = 1$. In this case only the 2-characteristic is impinging on the shock from the left, while only the 1-characteristic is impinging from the right. This shock is said to be *undercompressive*, because it only has two characteristics impinging rather than the three that one would normally expect for a nonlinear system of two equations. Note that it is also ambiguous whether we should call this a 1-shock or a 2-shock, since there is no single value of p for which $\lambda^p(q_l^*) > s > \lambda^p(q_r^*)$ as

we normally expect. This is again a consequence of the fact that the labeling of eigenvalues changes as we cross $u = v$, which can only happen where two eigenvalues are equal.

If we instead take the data

$$q_l = \begin{bmatrix} 5 \\ 4 \end{bmatrix}, \qquad q_r = \begin{bmatrix} 1 \\ 2 \end{bmatrix}, \tag{16.18}$$

then the Riemann solution is a shock in both u and v, moving together as a single shock for the system at speed $s = 3$. This is an *overcompressive shock*: in this case all four characteristics impinge on the shock.

16.3 Loss of Hyperbolicity

In order for a first-order system $q_t + f(q)_x = 0$ to be hyperbolic in the sense that we have used the term (more precisely, *strongly hyperbolic*), it is necessary that the Jacobian matrix $f'(q)$ be diagonalizable with real eigenvalues at each q in the physically relevant portion of state space. The system may fail to be hyperbolic at some point if the Jacobian matrix is not diagonalizable, which may happen if the eigenvalues are not distinct. Such a system is called *weakly hyperbolic* if the Jacobian matrix still has real eigenvalues. An example of this, in the context of a linear system, is given in Section 16.3.1. See Section 16.4.2 for a nonlinear example.

It may also happen that the Jacobian matrix is diagonalizable but has complex eigenvalues and is not hyperbolic at all. In some physical problems the equations are hyperbolic for most q but there are some *elliptic regions* of state space where the eigenvalues are complex. This case is discussed in Section 16.3.2.

16.3.1 A Weakly-hyperbolic System

In the examples of Section 16.2, the Jacobian matrix is still diagonalizable even though the eigenvalues are not distinct. When some eigenvalues are equal, it may also happen that the matrix is defective and fails to have a full set of m linearly independent eigenvectors. In this case the system is only weakly hyperbolic and the theory we have developed does not apply directly. However, it is interesting to consider what goes wrong in this case, as it gives additional insight into some aspects of the hyperbolic theory. There are also connections with the theory of hyperbolic equations with singular source terms, which will be studied again in Chapter 17.

Since a small perturbation of a nondiagonalizable matrix can yield one that is diagonalizable, one might wonder what happens if the problem is strongly hyperbolic but the matrix A is *nearly* nondiagonalizable. We should expect to observe some sort of singular behavior as we approach a nondiagonalizable matrix. Consider the system of equations

$$\begin{aligned} q_t^1 + uq_x^1 + \beta q_x^2 &= 0, \\ q_t^2 \qquad\quad + vq_x^2 &= 0, \end{aligned} \tag{16.19}$$

with the coefficient matrix

$$A = \begin{bmatrix} u & \beta \\ 0 & v \end{bmatrix}. \tag{16.20}$$

The eigenvalues are u and v and we assume that these are real numbers, along with the coupling coefficient β. If $u \neq v$, then the matrix is diagonalizable and the problem is hyperbolic. If $u = v$ then the problem is hyperbolic only if $\beta = 0$, in which case the system decouples into independent scalar advection equations for q^1 and q^2.

Suppose that $\beta \neq 0$ and that $v \leq u$. We will study the case $u \to v$. The eigenvalues and eigenvectors of A are

$$\begin{aligned} \lambda^1 &= v, & \lambda^2 &= u, \\ r^1 &= \begin{bmatrix} \beta \\ v-u \end{bmatrix}, & r^2 &= \begin{bmatrix} 1 \\ 0 \end{bmatrix}. \end{aligned} \tag{16.21}$$

Note that as $u \to v$, the eigenvector r^1 becomes collinear with r^2 and the eigenvector matrix R becomes singular:

$$R = \begin{bmatrix} \beta & 1 \\ v-u & 0 \end{bmatrix}, \qquad R^{-1} = \frac{1}{u-v}\begin{bmatrix} 0 & -1 \\ u-v & \beta \end{bmatrix} \quad \text{for } u \neq 0. \tag{16.22}$$

Based on the construction of Riemann solutions presented in Section 3.9, we see that solving the general Riemann problem with arbitrary states q_l and q_r will not be possible in the singular case $u = v$. Only if $q_r - q_l = \alpha^2 r^2$ for some scalar α^2 will we be able to find a solution. In this case $q_l^2 = q_r^2$ and so $q_x^2 \equiv 0$, and the system reduces to an advection equation for q^1 alone.

Now suppose $u = v + \epsilon$ with $\epsilon > 0$, so that the general Riemann problem can be solved by decomposing

$$q_r - q_l = \alpha^1 r^1 + \alpha^2 r^2.$$

Computing $\alpha = R^{-1}(q_r - q_l)$ yields

$$\begin{aligned} \alpha^1 &= -\frac{1}{\epsilon}\left(q_r^2 - q_l^2\right), \\ \alpha^2 &= q_r^1 - q_l^1 + \frac{\beta}{\epsilon}\left(q_r^2 - q_l^2\right). \end{aligned} \tag{16.23}$$

As $\epsilon \to 0$ the wave strengths blow up unless $q_l^2 = q_r^2$. The intermediate state is

$$q_m = q_l + \alpha^1 r^1 = \begin{bmatrix} q_l^1 - \beta\left(q_r^2 - q_l^2\right)/\epsilon \\ q_r^2 \end{bmatrix}, \tag{16.24}$$

as illustrated in Figure 16.7(a). As $\epsilon \to 0$ the eigendirections become collinear and $q_m^1 \to \infty$ (unless $q_r^2 = q_l^2$). Figure 16.7(b) shows the Riemann solution in the x–t plane, with $q = q_m$ only in the narrow wedge $v < x/t < v + \epsilon$. As the wave speeds coalesce, the solution blows

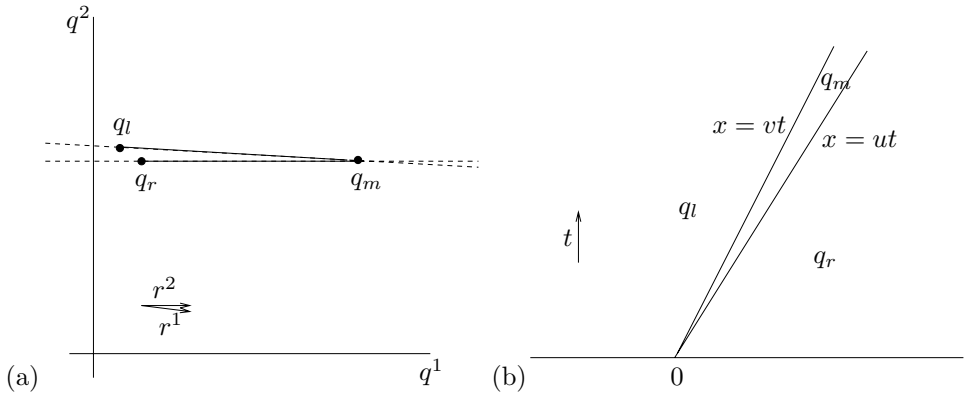

Fig. 16.7. Riemann solution for the case $\epsilon > 0$ but small: (a) in the phase plane, where the eigenvectors are nearly collinear; (b) in the x–t plane, where the wave speeds are nearly equal.

up in the neighborhood of $x = vt$. In the limit the solution can be viewed as consisting of a single jump discontinuity along with a delta-function singularity propagating at the same speed. The exact form of this distribution solution is derived in the next section. Similar phenomena are seen in some nonlinear problems, and are often called *singular shocks* or *delta shocks*. See [236], [239], [366], [441], [440] for some examples.

Singular-Source Interpretation

Another way to solve the Riemann problem for the system (16.19) is to note that the second equation does not depend on q^1 and can be easily solved to yield

$$q^2(x,t) = \overset{\circ}{q}{}^2(x - vt). \tag{16.25}$$

We can then view $\beta q_x^2(x,t) = \beta \overset{\circ}{q}{}_x^2(x - vt)$ as a known source term in the first equation of (16.19), resulting in

$$q_t^1 + uq_x^1 = -\beta \overset{\circ}{q}{}_x^2(x - vt). \tag{16.26}$$

For any known function $\psi(x,t)$, the solution to

$$q_t^1 + uq_x^1 = \psi(x,t) \tag{16.27}$$

is obtained by Duhamel's principle as

$$q^1(x,t) = \overset{\circ}{q}{}^1(x - ut) + \int_0^t \psi(x - u(t-\tau), \tau)\, d\tau. \tag{16.28}$$

Using $\psi(x,t) = -\beta \overset{\circ}{q}{}_x^2(x - vt)$ gives

$$q^1(x,t) = \overset{\circ}{q}{}^1(x - ut) - \beta \int_0^t \overset{\circ}{q}{}_x^2(x - ut + (u - v)\tau)\, d\tau. \tag{16.29}$$

If $u \neq v$ then the integral can be evaluated to give

$$q^1(x,t) = \mathring{q}^1(x-ut) - \frac{\beta}{u-v}[\mathring{q}^2(x-vt) - \mathring{q}^2(x-ut)]. \tag{16.30}$$

If $u = v$, then (16.29) reduces to

$$\begin{aligned} q^1(x,t) &= \mathring{q}^1(x-ut) - \beta \int_0^t \mathring{q}^2_x(x-vt)\,d\tau \\ &= \mathring{q}^1(x-ut) - \beta t \mathring{q}^2_x(x-vt). \end{aligned} \tag{16.31}$$

This result also follows from (16.30) on letting $u \to v$. If $\mathring{q}^2$ is a differentiable function, then this gives the general solution and the differential equation can be solved even in the case $u = v$, but note that in this case the solution grows with t in a manner unlike what we would expect from a hyperbolic equation.

Now consider the Riemann problem again, in which case $\mathring{q}^2$ is not differentiable at $x = 0$. If $u \neq v$, then the formula (16.30) still holds. Along with (16.25) this gives the solution to the Riemann problem, albeit in a different form than previously presented. If $u = v$ then (16.31) still holds if we interpret $\mathring{q}^2_x(x-vt)$ as a delta function. Writing the initial data in terms of the Heaviside function (3.28), we have

$$\mathring{q}^2(x) = q_l^2 + \big(q_r^2 - q_l^2\big)H(x) \quad \Longrightarrow \quad \mathring{q}^2_x(x-vt) = \big(q_r^2 - q_l^2\big)\delta(x-vt),$$

and hence

$$q^1(x,t) = q_l^1 + \big(q_r^1 - q_l^1\big)H(x-vt) - \beta t\big(q_r^2 - q_l^2\big)\delta(x-vt). \tag{16.32}$$

Note that this same form can be deduced from the Riemann structure shown in Figure 16.7(b), using the formula (16.24) and the observation that the solution q^1 has magnitude $-\beta(q_r^2 - q_l^2)/\epsilon$ over a region of width ϵt. As $\epsilon \to 0$ this approaches the delta function in (16.32).

Physical Interpretation

This Riemann problem has a simple physical interpretation if we take $v = 0$ and $u \geq 0$. Then $q^2(x,t) = \mathring{q}^2(x)$, and the equation (16.26) is an advection equation for q^1 with a delta function source at $x = 0$,

$$q_t^1 + uq_x^1 = D\delta(x), \tag{16.33}$$

where $D = -\beta(q_r^2 - q_l^2)$. This models the advection of a tracer in a pipe filled with fluid flowing at velocity u, with an isolated source of tracer at $x = 0$ (e.g., a contaminant leaking into the pipe at this point). For $u > 0$ the solution q^1 will have a jump discontinuity at $x = 0$, from q_l^1 to q_m^1, since the tracer advects only downstream and not upstream. The magnitude of the jump will depend on both D (the rate at which tracer is introduced at the source) and u (the rate at which it is carried downstream). For fixed D, larger values of u will lead to a smaller jump since the tracer is carried more rapidly away. As u decreases the magnitude of the jump will rise. As $u \to 0$ we approach the singular solution in which all the tracer

introduced at $x = 0$ remains at $x = 0$, yielding a delta function in the solution whose magnitude grows linearly with t, as seen in (16.32).

Similar analysis applies when $v \neq 0$, but now we must view the source location as propagating with velocity v rather than being fixed. In this case it is the relative speed $u - v$ that determines the magnitude of the jump in q^1, as already observed in the general Riemann solution.

16.3.2 Equations of Mixed Type

For some physical systems there are regions of state space where $f'(q)$ has complex eigenvalues. To see what this means, we first consider the linear system

$$\begin{bmatrix} p \\ u \end{bmatrix}_t + \begin{bmatrix} 0 & 1 \\ -1 & 0 \end{bmatrix} \begin{bmatrix} p \\ u \end{bmatrix}_x = 0. \tag{16.34}$$

This looks very similar to the acoustics equations (3.30) (with $u_0 = 0$ and $K_0 = \rho_0 = 1$), but has a crucial change in sign of one of the elements in the coefficient matrix A, resulting in complex eigenvalues $\lambda = \pm i$. The eigenvectors of A are also complex. Evidently we cannot use the techniques of Chapter 3 to solve this system, since it would not make sense physically to decompose the data into complex-valued waves moving at speeds $\pm i$.

We can combine the two equations in (16.34) and eliminate u by differentiating to obtain $p_{tt} = -u_{xt}$ and $u_{tx} = p_{xx}$, and hence

$$p_{tt} + p_{xx} = 0. \tag{16.35}$$

Going through this same process for the acoustics equations (with $+1$ in place of -1 in (16.34)) would result in the second-order wave equation $p_{tt} = p_{xx}$, as derived in Section 2.9.1. Here we instead obtain Laplace's equation (16.35), a second-order elliptic equation. From the theory of elliptic equations, it is known that this equation is well posed only if we specify boundary conditions for p on all boundaries of the region in x–t space where a solution is desired. This means that in order to solve the equation over some domain $[a, b] \times [0, T]$, we would not only have to specify initial data at time $t = 0$ and boundary data at $x = a$ and $x = b$, but also the solution at time T. This does not have the nature of a wave-propagation problem.

For a nonlinear problem it may happen that the Jacobian matrix $f'(q)$ has real eigenvalues at most points in state space but has complex eigenvalues over some relatively small region, called the *elliptic region* of state space. It is then an *equation of mixed type*. In this case it may be that wavelike solutions exist and the initial-value problem is well posed, at least for certain initial data, in spite of the elliptic region.

Problems of this sort often arise when studying wave propagation in materials that can undergo a *phase change*, for example from vapor to liquid. As discussed in Section 14.15, as a gas is compressed it is necessary eventually to consider the attractive intermolecular forces, leading to the van der Waals equation of state (14.66). If we consider the isothermal case where T is held constant, then we obtain the p-system (2.108) with the equation

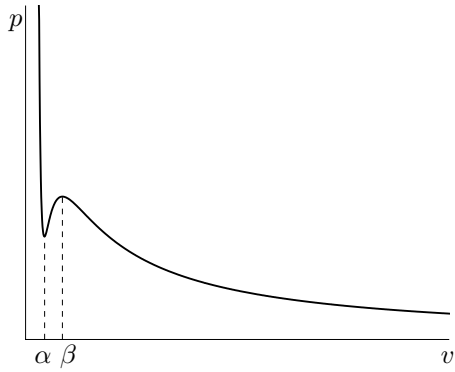

Fig. 16.8. The van der Waals equation of state (16.36).

of state

$$p(v) = \frac{RT}{v-b} - \frac{a}{v^2}, \tag{16.36}$$

where $v = 1/\rho$ is the specific volume. For sufficiently large temperature, this function is monotonically decreasing and the system is hyperbolic. If T is below the critical value $T_c = 8a/(27Rb)$, however, then the function $p(v)$ has the shape indicated in Figure 16.8. As the density increases (v decreases), the intermolecular forces are eventually sufficiently strong that the gas molecules begin to weakly bind to one another, and the gas changes phase and becomes a liquid. When v is sufficiently large it is pure gas (vapor phase) and p increases as v decreases as we expect in an ideal gas. However, as gas molecules begin to bind to one another, the gas pressure is reduced as a result, and so there is a region in which the pressure falls as v is decreased, the region $\alpha < v < \beta$ in Figure 16.8. For sufficiently small v the fluid is entirely liquid and decreasing v further leads to a strong increase in pressure.

Recall that for the p-system (2.108) the Jacobian matrix is

$$f'(q) = \begin{bmatrix} 0 & -1 \\ p'(v) & 0 \end{bmatrix}. \tag{16.37}$$

The eigenvalues $\pm\sqrt{-p'(v)}$ are real only where $p'(v) < 0$, and so the p–v state space has an elliptic region consisting of the strip $\alpha < v < \beta$, corresponding to the change of phase. We may wish to solve a Riemann problem in which the left and right states are in the two different phases in order to model the motion of the interface between phases. The solution will consist only of states that lie below α or above β, and so the solution essentially remains in the hyperbolic region, but it must include a phase-change jump across the elliptic region.

Even if the left and right states are both in the same phase, it is possible for the Riemann solution to involve states in the other phase. Consider, for example, the case where $v_l, v_r > \beta$ and $u_l > 0$ while $u_r < 0$, so that two gas streams are colliding. Then we expect the specific volume to decrease in the intermediate region after collision, which may lead to the liquid phase forming. In this case the Riemann solution might consist of two phase boundaries moving outward, in addition to shock waves in the gas phases. Similar equations arise in studying solids undergoing a phase transition.

The theory of such problems is beyond the scope of this book. Some other examples and further discussion may be found, for example, in [17], [26], [116], [130], [172], [200], [204], [213], [241], [269], [417], [418].

16.4 Spatially Varying Flux Functions

Chapter 9 contains a discussion of linear hyperbolic problems of the form $q_t + A(x)q_x = 0$ or $q_t + (A(x)q)_x = 0$, where the coefficient matrix $A(x)$ is spatially varying. For nonlinear problems we have thus far considered only the *autonomous* conservation law $q_t + f(q)_x = 0$, where the flux function $f(q)$ depends only on the solution q and is independent of x. If the flux function varies with x, then we have a conservation law of the form

$$q_t + f(q, x)_x = 0. \tag{16.38}$$

A system of this form arises, for example, when studying nonlinear elasticity in a heterogeneous medium where the stress–strain relation $\sigma(\epsilon, x)$ varies with x. See [273] for one application of a wave-propagation algorithm to this problem.

The flux function can be discretized to obtain a flux function $f_i(q)$ associated with the ith grid cell. The Riemann problem at $x_{i-1/2}$ now consists of the problem

$$\begin{aligned} q_t + f_{i-1}(q)_x &= 0 \quad \text{if } x < x_{i-1/2}, \\ q_t + f_i(q)_x &= 0 \quad \text{if } x > x_{i-1/2}, \end{aligned} \tag{16.39}$$

together with the data Q_{i-1} and Q_i. Often the Riemann solution is still a similarity solution of the form $q(x, t) = \tilde{q}(x/t)$ that in general consists of

- left-going waves, which must be shock or rarefaction waves relative to the flux function $f_{i-1}(q)$,
- right-going waves, which must be shock or rarefaction waves relative to the flux function $f_i(q)$,
- a stationary discontinuity at $x/t = 0$ between states $Q_l^{\Downarrow}$ and $Q_r^{\Downarrow}$ just to the left and right of this ray. In order for the solution to be bounded, the physical flux must be continuous across this ray and so

$$f_{i-1}(Q_l^{\Downarrow}) = f_i(Q_r^{\Downarrow}). \tag{16.40}$$

Solving the Riemann problem generally consists in finding states $Q_l^{\Downarrow}$ and $Q_r^{\Downarrow}$ satisfying (16.40) and having the property that Q_{i-1} can be connected to $Q_l^{\Downarrow}$ using only left-going waves, while $Q_r^{\Downarrow}$ can be connected to Q_i using only right-going waves. This cannot always be done, as it requires that there be a sufficient number of outgoing waves available. A simple example where it fails is the variable-coefficient advection equation (9.8) in the case where $u_{i-1} > 0$ and $u_i < 0$. All characteristics are approaching $x_{i-1/2}$, and the Riemann solution contains a delta function at this point rather than consisting only of waves.

For problems where the Riemann problem can be solved in terms of waves, the wave-propagation methods developed previously can be directly applied. Since the flux, unlike q, has no jump across $x_{i-1/2}$, this is often most easily done using the formulation of

Section 15.5. This requires only splitting the flux difference into propagating waves as in (15.74),

$$f_i(Q_i) - f_{i-1}(Q_{i-1}) = \sum_{p=1}^{m} \mathcal{Z}_{i-1/2}^p, \tag{16.41}$$

and often avoids the need to explicitly compute $Q_l^{\Downarrow}$ and $Q_r^{\Downarrow}$. For smooth solutions, this can be shown to be second-order accurate following the same approach as in Section 15.6. This method is explored in more detail in [18]. See [147], [148], [163], [243], [270], [288], [317], [361], [453] [460] for other examples of conservation laws with spatially varying fluxes and more discussion of numerical methods.

16.4.1 Traffic Flow with a Varying Speed Limit

The Riemann solution in the spatially varying case can have more complicated structure than in the autonomous case. As a simple scalar example, consider a traffic flow model that incorporates changes in the speed limit or visibility along the length of the highway. An equation of the form developed in Section 11.1 might then be used, but with a flux of the form

$$f(q, x) = u_{\max}(x)q(1 - q) \tag{16.42}$$

in place of (11.6). A linear version of this problem was discussed in Section 9.4.2. As in Chapter 9, a Riemann problem can now be formulated by specifying a piecewise constant function $u_{\max}(x)$ that jumps from $u_{\max,l}$ to $u_{\max,r}$ at $x = 0$, along with piecewise constant data q_l and q_r.

The two flux functions $f_l(q)$ and $f_r(q)$ are distinct quadratic functions as illustrated in Figure 16.9(a) for the case $u_{\max,l} = 2$ and $u_{\max,r} = 1$. This figure also indicates the structure of the Riemann solution for $q_l = 0.13$ and $q_r = 0.1$. The density as a function of x is shown in Figure 16.9(b) at time $t = 40$. The Riemann solution consists of a stationary jump from

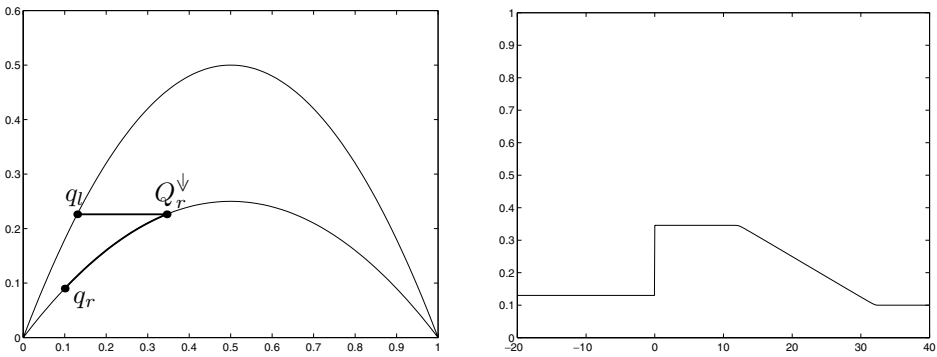

Fig. 16.9. Solution to the Riemann problem for traffic flow with a spatially varying flux function, with $q_l = 0.13$. (a) The flux functions $f_l(q) = 2q(1 - q)$ and $f_r(q) = q(1 - q)$ and the states arising in the Riemann solution. In this case $Q_l^{\Downarrow} = q_l$. (b) The density at $t = 40$. `[claw/book/chap16/vctraffic]`

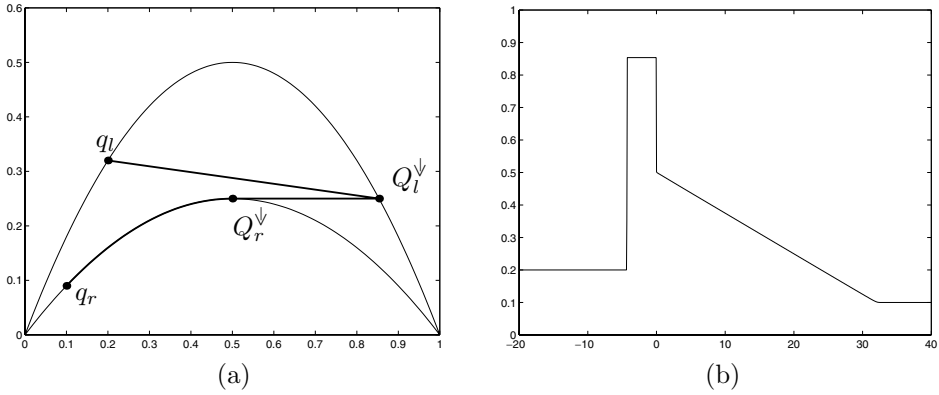

Fig. 16.10. Solution to the Riemann problem for traffic flow with a spatially varying flux function, with $q_l = 0.2$. (a) The flux functions $f_l(q) = 2q(1-q)$ and $f_r(q) = q(1-q)$ and the states arising in the Riemann solution. (b) The density at $t = 40$. `[claw/book/chap16/vctraffic]`

$q_l = Q_l^{\Downarrow}$ to a state $Q_r^{\Downarrow}$ at $x = 0$ along with a rarefaction wave from this state to q_r. In this case there is no left-going wave. The traffic slows down abruptly at the point $x = 0$ where the speed limit $u_{\max}$ decreases, and then speeds up again through a rarefaction wave to the state q_r. This is analogous to the example shown in Section 9.4.2, except that the right-going discontinuity becomes a rarefaction wave in the nonlinear case. Note that since we require (16.40), the jump from the flux curve $f_l(q)$ to $f_r(q)$ must occur along a horizontal line in Figure 16.9(a).

If the state q_l is increased above $0.5(1-\sqrt{0.5}) = 0.1464$, however, then a solution of the form seen in Figure 16.9(a) is no longer possible. The structure illustrated in Figure 16.10 is observed instead, shown here for $q_l = 0.2$. Upstream traffic is now sufficiently heavy that a shock wave forms and moves upstream, so that the Riemann solution contains a left-going shock and a right-going rarefaction wave, along with a stationary jump in density at $x = 0$ from $Q_l^{\Downarrow} = 0.5(1+\sqrt{0.5})$ to $Q_r^{\Downarrow} = 0.5$.

16.4.2 Rewriting the Equations as an Autonomous System

Some problems with spatially varying fluxes can be rewritten as larger autonomous systems of conservation laws by introducing new conserved variables that capture the spatial variation. For example, the scalar equation (16.38) with the spatially varying flux (16.42) can be rewritten as the following autonomous system of two equations:

$$\begin{aligned} q_t + (vq(1-q))_x &= 0, \\ v_t &= 0. \end{aligned} \tag{16.43}$$

The function $v(x,t)$ has zero flux and is constant in time, so if we choose $v(x,0) = u_{\max}(x)$, then we are solving the original problem.

The Jacobian matrix for the system (16.43) is

$$\begin{bmatrix} v(1-2q) & q(1-q) \\ 0 & 0 \end{bmatrix}. \tag{16.44}$$

The eigenvalues are $\lambda^1 = v(1-2q)$ (the characteristic speed expected from the original scalar equation) and $\lambda^2 = 0$ (the speed of stationary discontinuities at $x = 0$). But notice that this system is only weakly hyperbolic at $q = 0.5$, since the Jacobian is not diagonalizable at that point. This is related to the sudden change in structure of the Riemann solution shown in Figures 16.9 and 16.10 as $Q_r^{\Downarrow}$ reaches the value $q = 0.5$ and $Q_l^{\Downarrow}$ jumps from one root of a quadratic to the other. Note that the weak hyperbolicity at the one point $q = 0.5$ can lead to a Riemann solution that involves three waves (Figure 16.10) even though we have an autonomous system (16.43) of only two equations. This is another example of the sort of difficulty that can be caused by loss of strong hyperbolicity. See Exercise 13.11 for another example of this type of system.

16.5 Nonconservative Nonlinear Hyperbolic Equations

In Chapter 9 we considered nonconservative linear hyperbolic systems of the form $q_t + A(x)q_x = 0$, in the context of variable coefficient advection (the color equation, Section 9.3) and acoustics in a heterogeneous medium (Section 9.6). Solving the Riemann problem at the cell interface $x_{i-1/2}$ with matrices A_{i-1} and A_i yields waves and wave speeds that can be used in the wave-propagation form of the high-resolution algorithms, even though the equation is not in conservation form. In principle the same can be done for a general quasilinear hyperbolic equation of the form

$$q_t + A(q, x)q_x = 0. \tag{16.45}$$

If A depends explicitly on x, then we can first discretize $A(q, x)$ as we did for spatially varying flux functions in the previous section, to obtain a coefficient matrix $A_i(q)$ in the ith cell. Then the Riemann problem at $x_{i-1/2}$ consists of the data Q_{i-1}, Q_i and the equations

$$\begin{aligned} q_t + A_{i-1}(q)q_x &= 0 \quad \text{if } x < x_{i-1/2}, \\ q_t + A_i(q)q_x &= 0 \quad \text{if } x > x_{i-1/2}. \end{aligned} \tag{16.46}$$

If we can solve this Riemann problem to obtain physically meaningful waves and wave speeds, then the wave-propagation algorithm can be applied as usual. However, in the nonlinear case it may be difficult to determine the correct Riemann solution. This is true even in the autonomous case where there is no explicit dependence on x and the equation is simply

$$q_t + A(q)q_x = 0. \tag{16.47}$$

This differential equation only makes sense where q is differentiable. At discontinuities in q we have previously relied on the integral form of the conservation law to determine the resulting wave structure, using the Rankine–Hugoniot jump conditions. If the equation is not in conservation form, then we cannot use this for guidance.

Even for the simple Burgers equation, the quasilinear form $u_t + uu_x = 0$ is compatible with many different conservation laws, as discussed in Section 11.12. If we were only given the quasilinear equation to solve, it would not be clear what the correct wave speed is for a

shock wave. The nonconservative upwind method (12.25) can be viewed a a first-order wave-propagation method for the quasilinear problem using the wave speed $s^n_{i-1/2} = U^n_i$. This gives very different results (see Figure 12.5) than are obtained using $s^n_{i-1/2} = \frac{1}{2}(U^n_{i-1} + U^n_i)$, which yields the method (12.24).

If the quasilinear equation (16.47) can be rewritten as a physically meaningful conservation law (in particular, if q itself should be conserved and $A(q)$ is the Jacobian matrix of some flux function $f(q)$), then that conservation law should generally be solved rather than working with the quasilinear form numerically. However, in some applications a nonconservative equation is naturally obtained that does not have this property. In this case a detailed understanding of the physical problem is generally required in order to determine the proper structure of the Riemann solution.

Notice that if q is discontinuous at a point, then $A(q)$ is typically discontinuous there as well, while q_x contains a delta function singularity centered at this point. The theory of distributions can often be used to study equations involving delta functions and Heaviside functions, but the classical theory only allows these distributions to be multiplied by smooth functions. In (16.47) we have the product of a delta function q_x with a Heaviside function $A(q)$. Such products are generally ambiguous. If the delta function and the Heaviside function are each smoothed out slightly over width ϵ, for example by adding viscosity or diffusion to the problem, then we have ordinary continuous functions for which the product makes sense. But the limiting behavior as $\epsilon \to 0$ depends strongly on how each distribution is smoothed out. This general theory is beyond the scope of the present book. See [86], [87], [101], [194], [267], [268], [344], [345] for some further discussion and examples.

16.6 Nonconservative Transport Equations

One special nonconservative equation will be considered further here since it is easy to handle and often arises in practice. Consider a transport equation (or color equation) of the form

$$\phi_t + u\phi_x = 0 \tag{16.48}$$

for a tracer $\phi(x, t)$, and suppose that this equation is now coupled with a nonlinear system of m conservation laws that determines the velocity u. Then the full set of $m + 1$ equations is nonlinear, but is not in conservation form, because of (16.48). An example is given in Section 13.12.1, where the shallow water equations are considered along with a tracer ϕ used to distinguish fluid lying to the left and right of a contact discontinuity. In that case the equation (16.48) was rewritten in the conservation form (13.62) and a system of conservation laws obtained. However, in some applications it may be preferable to leave the transport equation in the nonconservative form (16.48). Otherwise one must recover ϕ by taking the ratio of the two conserved quantities $h\phi$ and h. This can lead to some numerical difficulties. In particular, if ϕ is expected to be piecewise constant whereas h and $h\phi$ are both spatially varying, then numerically the ratio $h\phi/h$ may not remain constant in regions where ϕ should be constant.

With the wave-propagation algorithms it is not necessary to put (16.48) into conservation form. In addition to the waves determined from solving the conservation laws for the fluid motion, we can simply add another wave $\mathcal{W}^{m+1}_{i-1/2}$ carrying the jump $\phi_i - \phi_{i-1}$ at speed

$s^{m+1}_{i-1/2} = u^-_{i-1} + u^+_i$ (as motivated by (9.17)). With this formulation, in regions where ϕ is constant we have $\mathcal{W}^{m+1}_{i-1/2} = 0$ and so ϕ will remain constant.

In the example of Section 13.12.1, the tracer is entirely passive and does not affect the fluid dynamics. It is often convenient to add a tracer of this form simply to track the motion of some portion of the fluid relative to the rest of the fluid. This can be very useful in flow visualization. Problems of this form also arise in tracking the movement of pollutants that are present in small quantities and do not affect the flow.

In other problems the value of ϕ may feed back into the fluid dynamics equations, leading to additional coupling between the equations. For example, consider a shock tube problem in which two different ideal polytropic gases (i.e., gamma-law gases with different values γ_l and γ_r) are initially separated by a membrane. Breaking the membrane gives a Riemann problem of the type mentioned in Section 14.15. To solve this problem numerically we must track the constituent gases. After the first time step there will generally be a grid cell that contains a mixture of the two gases (and many such cells in a multidimensional problem). In future time steps this mixing region will be further smeared out due to numerical diffusion in the method. If we let ϕ^n_i be the volume fraction of cell i that contains the left gas at time t_n, then ϕ satisfies the nonconservative transport equation (16.48). This equation must be coupled to the Euler equations (14.8), along with the equation of state (14.23),

$$E = \frac{p}{\gamma - 1} + \frac{1}{2}\rho u^2. \tag{16.49}$$

But now γ depends on ϕ. A cell that has volume fraction ϕ_i of gas l and volume fraction $1 - \phi_i$ of gas r has an effective value of γ_i that is related to γ_l and γ_r by

$$\frac{1}{\gamma_i - 1} = \frac{\phi_i}{\gamma_l - 1} + \frac{1 - \phi_i}{\gamma_r - 1}. \tag{16.50}$$

Rather than solving equation (16.48) for the volume fraction and then computing γ_i from (16.50), one can instead introduce a new variable

$$G = \frac{1}{\gamma - 1} \tag{16.51}$$

and couple the Euler equations to a transport equation for G,

$$G_t + uG_x = 0. \tag{16.52}$$

The equation of state then becomes

$$E = Gp + \frac{1}{2}\rho u^2. \tag{16.53}$$

Note that by using the nonconservative equation (16.52), we insure that G and hence γ will remain constant numerically in regions where there is only a single gas present. Using the continuity equation $\rho_t + (\rho u)_x = 0$ would allow us to rewrite (16.52) as

$$(\rho G)_t + (\rho u G)_x = 0, \tag{16.54}$$

but using this form introduces the possibility that $G = (\rho G)/\rho$ will vary numerically due to variations in ρ and the fact that ρ and ρG both contain numerical errors.

It is also important to transport a quantity such as ϕ or G for which the transport equation continues to be valid in the context of cell averages and numerical diffusion. It is tempting to simply use the transport equation

$$\gamma_t + u\gamma_x = 0 \tag{16.55}$$

to advect γ with the flow. This equation does hold for diffusionless gases where no mixing occurs, since γ will then always be either γ_l or γ_r and the contact discontinuity is simply advected with the flow. But numerically the gases do mix, and so (16.52) must be used instead.

If (16.55) is used numerically, then pressure oscillations will typically develop near the interface between gases, in spite of the fact that the pressure should be constant across the contact discontinuity. This results from using the wrong equation of state (i.e., the wrong value of γ) in the mixture of gases generated by numerical diffusion. For more discussion of these issues and some numerical examples, see [4], [5], [71], [131], [132], [218], [231], [259], [362], [394], [388], [395], [412], [452].

Exercises

16.1. Determine the entropy-satisfying solution to the Riemann problem for the scalar conservation law $q_t + f(q)_x = 0$ for the following nonconvex flux functions and data. In each case also sketch the characteristics and the structure of the Riemann solution in the x–t plane.
   (a) $f(q) = q^3, q_l = 0, q_r = 2,$
   (b) $f(q) = q^3, q_l = 2, q_r = -1,$

16.2. Use the equal area rule to find an expression for the shock location in the Buckley–Leverett equation, as a function of t. Verify that the Rankine–Hugoniot condition is always satisfied and that the shock propagates at a constant speed that agrees with the speed $f(q^*)/q^*$ determined from the convex-hull construction.

16.3. For the Buckley–Leverett equation, show that (16.4) is violated if the shock goes above q^*.

16.4. Explain why it is impossible to have a Riemann solution involving both a shock and a rarefaction when f is convex or concave.

16.5. For the nonstrictly hyperbolic system of equations (16.13) with data (16.17), plot the following:
   (a) the solution to the Riemann problem in state space,
   (b) the 1-characteristics and 2-characteristics in the x–t plane for this solution, as in the plots of Figure 13.6, for example.

16.6. Repeat Exercise 16.5 for the data (16.18).

16.7. (a) Determine the eigenvectors of the Jacobian matrix (16.44), and sketch the integral curves of each eigenvector in state space (the q–v plane).
   (b) Sketch the solutions to the Riemann problems shown in Figures 16.9 and 16.10 in state space.